Biochimica et Biophysica Acta 1858 (2016) 1944–1953

Contents lists available at ScienceDirect

Biochimica et Biophysica Acta

journal homepage: www.elsevier.com/locate/bbamem

# Relationship between intracellular calcium and morphologic changes in rabbit erythrocytes: Effects of the acylated and unacylated forms of *E. coli* alpha-hemolysin

Romina F. Vázquez [a], Sabina M. Maté [a], Laura S. Bakás [b], Carlos Muñoz-Garay [c], Vanesa S. Herlax [a,*]

[a] Instituto de Investigaciones Bioquímicas de La Plata (INIBIOLP), CCT- La Plata, CONICET, Facultad de Ciencias Médicas, Universidad Nacional de La Plata, 60 y 120, 1900 La Plata, Argentina
[b] Departamento de Ciencias Biológicas, Facultad de Ciencias Exactas, Universidad Nacional de La Plata, 47 y 115, 1900 La Plata, Argentina
[c] Instituto de Ciencias Físicas, Universidad Nacional Autónoma de México (UNAM), Av. Universidad 2001, Col. Chamilpa, 62210 Cuernavaca, Mexico

ARTICLE INFO

*Article history:*
Received 14 January 2016
Received in revised form 15 April 2016
Accepted 16 May 2016
Available online 17 May 2016

*Keywords:*
RTX toxins
HlyA
Calcium
Purinergic receptors
Unacylated protein
Exovesicles
Discocyte-echinocyte-spherocyte transition

ABSTRACT

Alpha-hemolysin (HlyA) is a hemolytic and cytotoxic protein secreted by uropathogenic *Escherichia coli* strains, whose expression correlates with the severity of the infections produced. HlyA is synthesized as a protoxin, ProHlyA, that becomes matured to the active form in the cytosol by hemolysin-C–directed fatty acylation at the ε-amino residues of Lys 564 and Lys 690, before export from the toxin-producing bacteria. This posttranslational modification is remarkable because the nature of the protein is changed by the lipidic moiety from a benign protein to a frank toxin.

In the present work, we demonstrated for the first time that, despite being hemolitically inactive, ProHlyA induced cellular morphologic changes in rabbit erythrocytes. A discocyte-to-echinocyte transformation was triggered by the protoxin in the absence of any accompanying increase in intracellular-$Ca^{2+}$ levels. In addition, the $Ca^{2+}$-influx kinetics in HlyA-treated erythrocytes indicated that the active toxin induced an elevation in intraerythrocyte-$Ca^{2+}$ content in a biphasic manner, with an initial rise in $Ca^{2+}$ that depended on the association of the protein with the target membrane and a second increment corresponding to an activation of purinergic channels. The first increase was sufficient to trigger a discocyte-echinocyte-spherocyte transition in erythrocyte shape, though the subsequent rise mediated by purinergic signalling was essential for the occurrence of hemolysis. The results presented here provide new insights into the mechanism of action of this toxin.



## 1. Introduction

Alpha hemolysin (HlyA) is a hemolytic and cytotoxic protein secreted by the uropathogenic strains of *Escherichia coli*. This toxin is active against a broad range of species and cell types. Quantification of HlyA phenotypes among commensal *E. coli* isolates revealed that 15% encode HlyA; with the degree of expression of that gene correlating with the severity of infection, as up to 78% of the uropathogenic-*E. coli* isolates from pyelonephritis cases express this toxin [1,2].

HlyA represents the prototype of a wide range of toxins referred to as the RTX-toxin family (*i. e.*, Repeat in toxin). Produced by a variety of Gram-negative bacteria, these proteins exhibit two common features. The first is the presence of arrays of glycine- and aspartate-rich nonapeptide repeats, which sequences are located at the C-terminus. The second is the unique mode of secretion via the type-I system (an ABC-binding–cassette transporter) [3–5]. The RTX-operon arrangement of the genes required for HlyA expression, activation, and secretion is *hlyCABD*, with the *tolC* gene at an independent locus [6–9]. The HlyC protein is an acyltransferase required for the activation of HlyA in the bacterial cytosol before the toxin's secretion. HlyA is initially synthesized as a protoxin (ProHlyA), with its activation consisting in a post-translational modification of the ε-amino groups of internal lysine residues by amide-linkage to fatty-acyl moieties. The mechanism of this novel type of protein acylation has been extensively analyzed for HlyA [8,10]. HlyC uses the fatty-acyl residues carried by the acylcarrier protein to form a covalent acyl-HlyC intermediate, which species then transfers the fatty-acyl residues to the ε-amino groups of the Lys 564 and Lys 690 residues of ProHlyA [11,12]. Acylation is not required for membrane binding, but the lipidic modification is essential for the subsequent lysis of the target cells [13,14]. This posttranslational alteration is remarkable in that the behavior of the protein becomes changed through this lipidic linkage from a benign protein to a frank toxin—with that part of the transformation being an especially unusual mechanism in prokaryotes since in only a few eukaryotic proteins is this type of acylation found [15].

* Corresponding author: INIBIOLP, Facultad de Ciencias Médicas, Universidad Nacional de La Plata, 60 y 120, 1900 La Plata, Argentina.
*E-mail address:* vherlax@med.unlp.edu.ar (V.S. Herlax).

http://dx.doi.org/10.1016/j.bbamem.2016.05.013
0005-2736/

Many studies aimed at elucidating the mechanism of action of HlyA have been conducted with erythrocytes as target cells [13,16–18], to cite but a few. In recent years, Skals et al. introduced the idea of how autocrine and paracrine signalling along with the cell's intrinsic volume regulation markedly influences the fate of erythrocytes after membrane interaction with HlyA [19–21]. Those authors demonstrated with equine, murine, and human erythrocytes that cellular-ATP leakage and $Ca^{2+}$ influxes through the interaction of HlyA activate purinergic receptors and pannexin channels [20]. This activation further potentiates the influx of extracellular $Ca^{2+}$ and contributes to the shrinkage and crenation of erythrocytes that result from the activation of $Ca^{2+}$-dependent $K^+$ channels (*i. e.*, the Gardos $K^+$-specific channels) and the Ca-activated $Cl^-$ channel TMEM16A [19]. This intracellular-$Ca^{2+}$ increase also activates the calpain neutral proteases that hydrolyze cytoskeletal proteins, thus contributing to changes in the erythrocyte morphology [22]. Recently, we were able to quantify the intracellular-$Ca^{2+}$ concentration in rabbit erythrocytes treated with HlyA by fluorescence lifetime-imaging microscopy [23]. By that technique, we demonstrated that intracellular $Ca^{2+}$ increases fourfold in HlyA-treated erythrocytes before the occurrence of hemolysis—and in a biphasic manner—suggesting that different mechanisms were involved in the rise in $Ca^{2+}$.

In view of these considerations, the present work focussed on the interaction of the unacylated form of HlyA (*i. e.*, the ProHlyA) with rabbit erythrocytes by monitoring cell morphology and the intraerythrocyte-$Ca^{2+}$ levels after treatment with the toxin. Microscopical imaging and flow-cytometry demonstrated that although ProHlyA causes neither $Ca^{2+}$ influx nor the lysis of rabbit erythrocytes, that protoxin induces cellular morphologic alterations. These changes could be caused by the association of the protein with the erythrocyte membrane since the unacylated inactive protein precursor produces the same effects in terms of increments in the surface pressure of lipid monolayers mimicking the outer leaflet of rabbit-erythrocyte membranes as does the active HlyA. These findings provide new insights into the mechanism of action of the active toxin HlyA.

## 2. Materials and methods

### 2.1. Materials

HlyA and ProHlyA were purified from culture filtrates of the *E. coli* strains WAM 1824 [24] and WAM 783 [18], respectively, following the procedure described previously [25].

Lipids, 1,2-dioleoyl-*sn*-glycero-3-phosphocholine (DOPC), *N*-palmitoyl-D-*erythro*-sphingosylphosphorylcholine (16:0-SM), and cholesterol (Chol), were purchased from Avanti Polar Lipids (Birmingham, AL, USA); Fluo-4 acetoxymethyl ester (AM), from Molecular Probes, Inc. (Eugene, OR, USA), and ionomycin, bovine serum albumin, Brilliant Blue G (BBG), $NiCl_2$, and the other reagents, unless indicated to the contrary, from Sigma-Aldrich (St. Louis, MO, USA). The HEPES- [4-(2-hydroxyethyl)-1-piperazineethanesulfonic acid-] buffered saline (HBS) contained (in mM): 135 NaCl, 10 HEPES, 5.3 KCl, 2.0 $CaCl_2$, 1.0 $MgSO_4$, 5.0 glucose, pH 7.4.

### 2.2. Erythrocyte preparation

Blood samples were obtained at the laboratory-animal facility of the Instituto de Biotecnología, UNAM, in strict accordance with the technical specifications of the Mexican Official Standard NOM-062-ZOO-1999 and the international ethical guidelines for the care and use of laboratory animals.

Blood from healthy rabbits was obtained by venipuncture and anticoagulated by manual defibrination. The total erythrocyte population was separated from other blood components by centrifugation at 1500*g* for 10 min at 15 °C and washed three times by centrifuging with 0.9% (w/v) NaCl. After the last wash, the packed erythrocytes were resuspended in Alsever's solution (Sigma Chemical Co., St. Louis, MO, USA) and stored at 4 °C. The erythrocytes were used within the first two days after extraction.

### 2.3. Hemolytic assays

Measurements of hemolytic activity were performed by adding 100 μl of a 2% (v/v) erythrocyte suspension in HBS buffer to 100 μl of toxin dilutions in a microtiter plate. After 30 min at 37 °C, the plates were centrifuged and the hemolysis quantified as released hemoglobin by measuring the absorbance at 412 nm.

For the lysis-inhibition assays erythrocyte suspensions were pretreated with 4.0 mM $NiCl_2$ or 20 μM BBG in HBS buffer for 30 min at 37 °C. Then 100 μl of these suspensions were added to the toxin dilutions to perform the hemolytic assays.

For measuring the hemolytic activity of ProHlyA in the presence of ATP, HBS buffer containing 6.0 or 2.0 mM of ATP, pH 7.4, was used to prepare the protein dilutions. Then the erythrocyte suspension in HBS was added to each well as stated above to perform the assays.

### 2.4. Live-cell imaging

Erythrocytes were attached to glass coverslips mounted on custom-made imaging chambers by sedimentation from 0.02% (v/v) suspensions for 5 min. For intracellular-$Ca^{2+}$ imaging, erythrocyte suspensions (1% [v/v]) were incubated with Fluo-4 AM (1 μM) for 60 min at 37 °C with constant gentle stirring in the dark. The cells were next washed twice, resuspended in HBS buffer, and then attached to the coverslips. In all these experiments 0.05% (w/v) bovine-serum albumin was added to the buffer to avoid crenation of the erythrocytes as they came in contact with the glass [26].

Imaging chambers were placed on the stage of an Eclipse TE2000U microscope (Nikon Instruments, Melville, NY, USA). Erythrocytes were imaged with a CFI Apo TIRF 60×/1.49 N.A., oil-immersion objective (Nikon) and an iXon Ultra 897 EMCCD camera (Andor Technology, Belfast, NIR, UK). A blue light-emitting diode (470 nm) powered by OptoLED, both from Cairn Research Company (Faversham, Kent, UK), and a filter set of HQ480/40× for excitation and of D535/40 m for emission (Chroma Technology, Rockingham, VT, USA) were employed to measure the Fluo-4 fluorescence. Images were captured through the use of the Andor iQ software (Andor Technology). Time-lapse recordings of the erythrocyte morphology or Fluo-4 fluorescence were collected at different times after the addition of HlyA or ProHlyA at a sampling rate of 0.1 Hz. The same technical set up was used for experiments in the presence of 2 mM $NiCl_2$ or 10 μM BBG.

Changes in erythrocyte-fluorescence intensity were calculated by marking regions of interest around the cells by means of ImageJ software [27]. The mean fluorescence intensity was measured for individual cells at each time point and the values corrected by subtracting the mean fluorescence in the background of that region at the same instant.

### 2.5. Analyses on the ImageStream® MkII Imaging Flow Cytometer

A 0.5% (v/v) suspension of erythrocytes loaded with Fluo-4 AM (5 μM) was treated with 70 and 7 nM of ProHlyA and HlyA, respectively. Image acquisition and analysis were performed on an ImageStream® MkII imaging cytometer, through the use of INSPIRE software. The instrument and software were set up as follows: Channels 01 (bright field), 02 (fluorescence channel) and channel 12 (scattering channel). The magnification was 60×, providing a pixel size of 0.3 $\mu m^2$, while the lasers 488 and 745 were activated for fluorescence and side-scatter, respectively. The acquisition cut-off was set to 10,000. The analysis of the data was performed by means of the IDEAS software (Amnis Corp., Seattle, WA, USA).

### 2.6. Monolayer experiments

Surface-pressure experiments were carried out with a KSV NIMA Langmuir-trough Model 102A (KSV-NIMA Biolin Scientific, Espoo, Finland) with a Wilhelmy platinum plate as the surface-pressure sensor. The aqueous subphase consisted of (in mM) 20 Tris, 150 NaCl, pH 7.4 (TC Buffer) plus 2.0 $CaCl_2$. The ternary lipid mixture DOPC/16:0-SM/Chol at a 2:1:1 molar ratio dissolved in chloroform was gently spread over the surface of a Teflon microtrough containing only 300 μl of subphase until the desired initial surface pressure was attained. HlyA or ProHlyA at 40 nM final concentration were then injected into the subphase bulk with a micropipette. The increment in surface pressure *versus* time was recorded until a stable signal was obtained. All the experiments were carried out at 20 ± 1 °C.

### 2.7. Statistical analysis

The Student *t*-test was used for statistical comparisons among the groups and differences were considered statistically significant when $p < 0.05$ ($^{*}p < 0.05$, $^{**}p < 0.01$, $^{***}p < 0.001$).

## 3. Results

### 3.1. Morphologic changes of erythrocytes treated with HlyA and ProHlyA

Many experiments have been carried out with erythrocytes from different animal species in order to study the lytic mechanism of HlyA [17,19,28,29]; nevertheless, beyond the nonhemolytic activity reported for ProHlyA, the effect of this unacylated precursor on erythrocytes has been poorly investigated. In view of this shortcoming, the action of both proteins, HlyA and ProHlyA, were accordingly studied in rabbit erythrocytes. Fig. 1, Panel A depicts the hemolysis of 2% (v/v) of rabbit-erythrocyte suspensions treated with HlyA and ProHlyA. As had been previously demonstrated, HlyA effectively lysed erythrocytes in a dose-dependent fashion, but ProHlyA produced no hemolysis at any concentration tested. When hemolysis was monitored by optical microscopy, morphologic changes were observed in HlyA- and also, quite strikingly, in ProHlyA-treated cells (Fig. 1, Panel B). Microscopy was performed over time after treatment with 5 nM of HlyA ($n = 4$ from 2 blood samples). At this toxin concentration an erythrocyte lysis of 75% was observed after 40 min (Fig. 1, Panel C). HlyA induced first the crenation of these rabbit erythrocytes, followed by a swelling and lysis of the

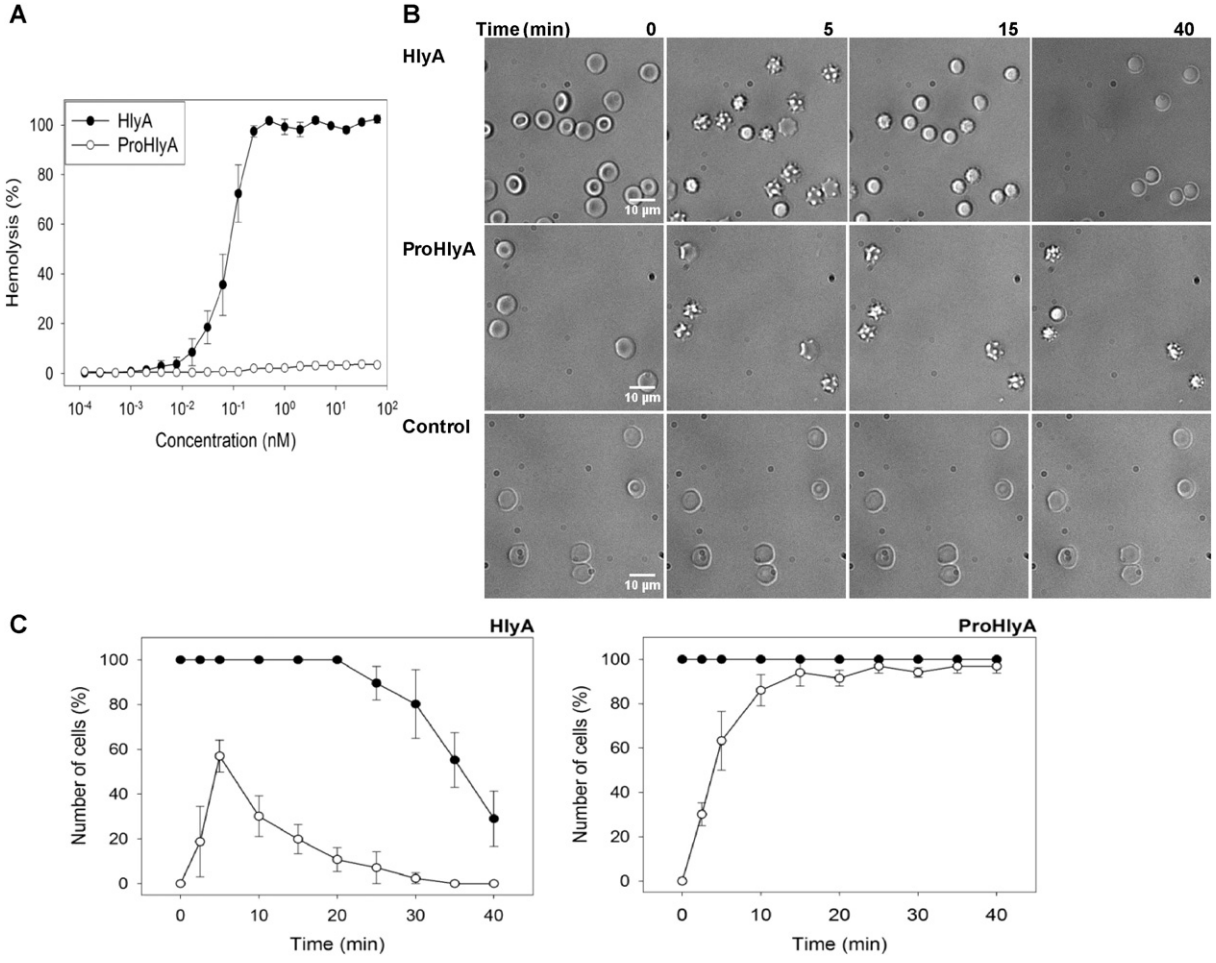


**Fig. 1.** Hemolytic activity of HlyA and ProHlyA in rabbit erythrocytes. Panel A: The hemolysis of HlyA and ProHlyA was measured as the hemoglobin released after a 30-min exposure to different concentrations of the proteins. In the figure, the percent hemolysis is plotted on the *ordinate* as an exponential function of the concentration of protein in nM on the *abscissa*. Filled circles, HlyA; open circles, ProHlyA. The data represent the mean ± SEM of 3 independent experiments with blood from 3 different animals. Panel B: Representative bright-field images of erythrocytes taken before (time 0) and 5, 15, or 40 min (indicated above the figure) after the addition of 5 nM of HlyA (upper row) or 50 nM of ProHlyA (middle row). The images corresponding to control erythrocytes (lower row) pertain to the same time points after the addition of a volume of buffer equal to that added to the HlyA and ProHlyA samples, but without the protein. Panel C: Percentage of unlysed cells (filled circles) and crenated cells (open circles) at different times after the addition of 5 nM HlyA (left figure) or 50 nM ProHlyA (right figure). Bright-field images were analyzed over time after exposure to the proteins to assess the cell counts. In the figures the percentage of cells in either condition is plotted on the *ordinate* as a function of time in min on the *abscissa*. The data represent the means ± SEM of $n = 4$ images for each time point corresponding to independent experiments with blood from 2 different animals.

cells, as had been previously described in human erythrocytes by Skals et al. [19,20]. When the same concentration of ProHlyA was tested, morphologic changes were also observed, but at longer time intervals (not shown). In contrast, when the concentration of the protoxin was increased by tenfold over that used with HlyA, ProHlyA induced an initial crenation of the erythrocytes within 5 min, with this alteration reaching 100% within 10 min. No further changes in morphology, however, were observed thereafter, as the erythrocytes remained mostly in an echinocytic shape over time and neither swelled nor lysed (Fig. 1, Panels B and C). Images of the control erythrocytes were taken over the same time course, thus confirming that these changes were caused by the HlyA or ProHlyA treatment since no such morphologic alterations were observed in the absence of those proteins (Fig. 1, Panel B). These findings indicate that, unlike what would have been expected from previous results, the interaction of ProHlyA with erythrocyte membranes may trigger cellular responses that lead to morphologic changes in the cell even though those responses do not produce lysis.

### 3.2. Measurement of intracellular-$Ca^{2+}$ levels in HlyA- and ProHlyA-treated erythrocytes

Skals et al. postulated that the induction of shrinkage in human erythrocytes produced by HlyA resulted from the activation of $Ca^{2+}$-activated $K^+$ channels (*i. e.*, the Gardos channels) [19]. In agreement with this proposal, we had previously observed an increment in intraerythrocyte-$Ca^{2+}$ levels occurring before the hemolysis of rabbit erythrocytes treated with HlyA that could explain the shrinkage found in those HlyA-treated cells. Therefore, in order to investigate if $Ca^{2+}$ ions were involved in the discocyte-to-echinocyte–shape transition found in ProHlyA-treated cells, we monitored the influx of $Ca^{2+}$ in Fluo-4–loaded rabbit erythrocytes after treatment with ProHlyA or HlyA. Fig. 2, Panel A illustrates how an HlyA-induced increase in $Ca^{2+}$ levels occurs in a biphasic manner, as we had demonstrated previously [23]. An initial sharp elevation was observed within 5 to 8 min of HlyA interaction with the erythrocytes. Then a slower, sustained rise followed until the point of cellular hemolysis after 25–35 min. This pattern is in agreement with the data presented in Fig. 1, Panel C, where a 50% decay in the number of erythrocytes was observed after 35 min of exposure to HlyA. In contrast, ProHlyA induced no intracellular-$Ca^{2+}$ increase whatsoever (Fig. 2, Panels A–C). Since the ProHlyA-induced crenation of the erythrocytes was independent of an increase in $Ca^{2+}$, responses other than Gardos-channel activation must be involved in the morphologic changes observed. Furthermore, when the HlyA hemolytic activity was monitored in $Ca^{2+}$-free buffer (10 mM HEPES, 150 mM NaCl, 5 mM EDTA, pH 7.4), the same behavior as seen with ProHlyA was observed (Fig. 2, Panel D). Under these conditions, the rabbit erythrocytes likewise became transformed from the discocyte to the echinocyte shape and remained in that morphology thereafter in the

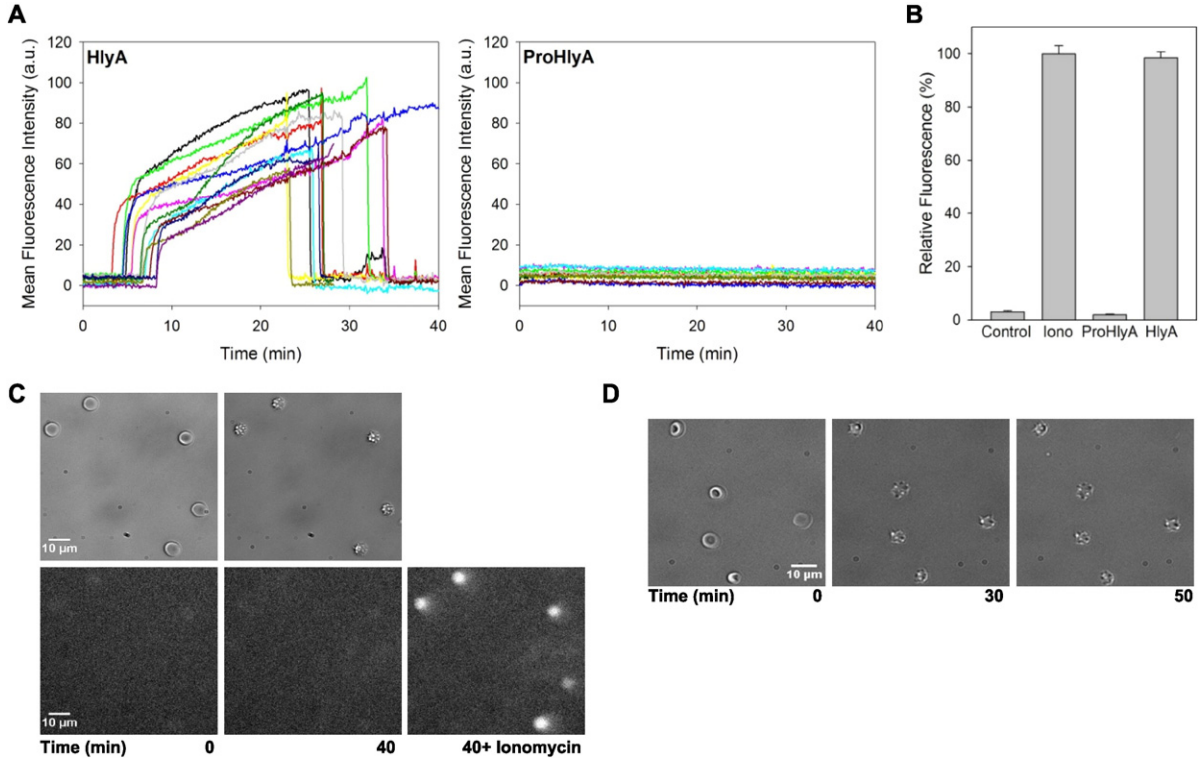


**Fig 2.** Calcium influx in HlyA- or ProHlyA-treated erythrocytes. Panel A: Changes in intracellular-$Ca^{2+}$ levels in single cells in response to 5 nM HlyA (left figure) or 50 nM ProHlyA (right figure) as visualized by fluorescence imaging of the $Ca^{2+}$ sensor Fluo-4 (excitation at 470 nm; emission at 535/40 nm). In the figures, the mean fluorescence intensity in arbitrary units (a. u.) per cell is plotted on the *ordinate* as a function of time in min on the *abscissa*. Each figure shows representative records obtained in single cells (colored curves) in a time-course analysis of fluorescence images through the use of ImageJ software as described in Materials and methods. Panel B: The bar graphs plot on the *ordinate* the average increment in mean fluorescence intensity of untreated cells (Control, N = 83) and of ProHlyA- (N = 98), or HlyA- (N = 128) treated cells normalized with respect to the average elevation observed for ionomycin-treated cells (Iono, N = 87) set as a 100% increase. For Control and ProHlyA treatment, the rise in fluorescence intensity increase was measured after 40 min of image acquisition. For HlyA-treated cells the elevation was measured at the maximum of fluorescence intensity observed, just before the occurrence of hemolysis. The data represent the mean values ± SEM from 5 independent experiments with blood from 3 different animals. Panel C: Bright-field (upper row) and fluorescence-intensity (lower row) images before (time 0, left fields) and 40 min (right fields) after the addition of 50 nM ProHlyA. An image of the same sample after a 40-min exposure to ProHlyA with the subsequent addition of a 1 µM final concentration of ionomycin is also shown as the fluorescence-positive control for Fluo-4–loaded cells (adjacent right fields). Panel D: Images of erythrocytes in $Ca^{2+}$-free buffer before (time 0) and after the addition of 10 nM HlyA (at 30 and 50 min, indicated below the figure). The images as well as the fluorescence kinetics are representative of >5 independent experiments for each of the two proteins with blood obtained from 3 different rabbits.

absence of any cell lysis, thus confirming the notion that $Ca^{2+}$ entry is not strictly necessary for erythrocyte crenation to occur under the influence of the toxin.

With the aim at studying further the relationship between increases in intracellular $Ca^{2+}$ and morphologic changes in HlyA- and ProHlyA-treated erythrocytes, we performed flow-cytometry analysis in an *ImageStream® MkII Imaging Flow Cytometer* since this technology had the overwhelming advantage of allowing the observation of each individual event passing through the flow cell. Fig. 3 shows the histograms of fluorescence intensity corresponding to Fluo-4–loaded rabbit erythrocytes at different times after treatment with both proteins. The figure clearly shows that ProHlyA induced cellular morphologic alterations involving a conversion of the erythrocytes to an echinocytic shape even though no increment in fluorescence was observed, thus reconfirming the results obtained by fluorescence-microscopy imaging. The histograms corresponding to HlyA-treated erythrocytes indicated the presence of different populations of cells differing in their fluorescence intensity. The group of cells with the highest fluorescence intensity (similar to that observed for ionomycin-treated erythrocytes) corresponded to spherocytes, as visualized in the bright-field channel (*cf.* the upper *insets* in the figures), while the population with intermediate fluorescence intensity corresponded to echinocytic cells (the lower *insets* in the figures). After 40 min of exposure to HlyA, a third population appeared with a very low fluorescence intensity that could be attributed to erythrocyte ghosts (the lowest *inset* in that figure). We do, however, recognize that because Fluo-4 is a nonratiometric $Ca^{2+}$ indicator, the fluorescence-intensity emission observed could be affected by the cellular morphologic changes occurring in the treated erythrocytes *per se* since both the $Ca^{2+}$-ion and the Fluo-4 concentrations could be modified as a result of the accompanying volume changes.

Fig. 4 shows a scatter plot of channel-02–fluorescence intensity plotted against the area for each cell treated for 40 min with ProHlyA or HlyA. The echinocyte population depicted for HlyA in Fig. 3, occupies a slightly smaller area than the control erythrocytes, which area is similar to the area of echinocytes induced by ProHlyA, but the fluorescence intensity of the former is nearly twofold higher than that of the latter (Fig. 4). This feature could account for the rapid series of steps that take place after HlyA treatment, where certainly a number of these echinocytes might have already started the transformation to spherocytes as a result of $Ca^{2+}$ entry. That, however, ProHlyA-treated erythrocytes, which population remained as echinocytes over time, maintained their fluorescence-intensity level similar to those of the control cells is indeed noteworthy. In contrast, in the HlyA-treated erythrocytes, the cell population with a high fluorescence intensity corresponding to spherocytes, showed a significant reduction in area (15%) compared to control erythrocytes and crenated cells. The same characteristic was found in erythrocytes after addition of ionomycin confirming that the echinocyte-to-spherocyte–shape transition is accompanied by a reduction in cell dimensions. Moreover, erythrocyte ghosts which appeared as a result of cell lysis also exhibited very low areas.

According to a recent report, purinergic amplification is needed for lysis of HlyA-treated erythrocytes since different P2-channel blockers abrogate hemolysis in human, murine and equine red-blood cells [20]. Considering this finding, we monitored the hemolytic activity in rabbit erythrocytes after HlyA addition in the presence of $Ca^{2+}$-channel blockers. Accordingly, the voltage-gated–$Ca^{2+}$-channel blocker $Ni^{2+}$ and the P2-receptor antagonist BBG, both impaired HlyA lytic activity in rabbit erythrocytes (Fig. 5, Panel A). Therefore, after treatment of rabbit erythrocytes with HlyA in the presence of those channel blockers, and thus under nonhemolytic conditions, cell morphology and $Ca^{2+}$ levels were monitored in order to compare those responses with the corresponding behavior in ProHlyA-treated erythrocytes. Bright-field microscopy revealed that under these conditions the erythrocytes still underwent the discocyte-echinocyte-spherocyte–shape-transformation sequence although the cells remained as spherocytes and did not swell or lyse (Fig. 5, Panel C). Furthermore, when $Ca^{2+}$-influx kinetics were analyzed by the Fluo-4 imaging of HlyA-treated erythrocytes in the presence of these inhibitors, an increase in intraerythrocyte-$Ca^{2+}$ levels was still observed, though not following biphasic kinetics as before (*cf* Fig. 2, Panel A) but instead involving only the first rise in intracellular

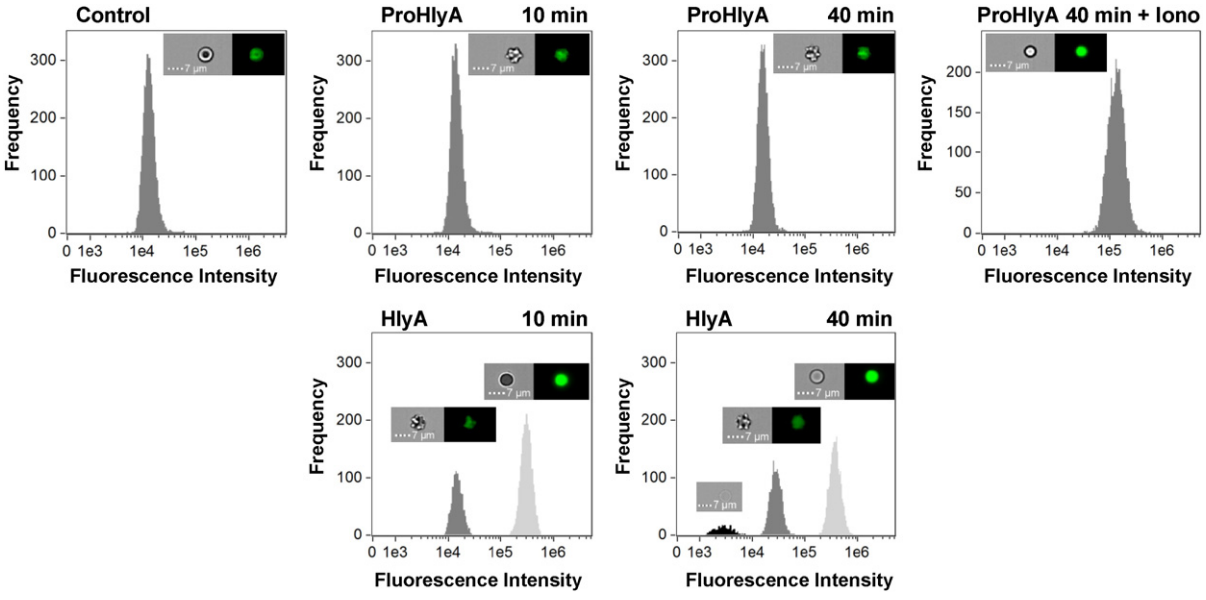


**Fig. 3.** Flow-cytometry analysis of HlyA- and ProHlyA-treated rabbit erythrocytes. Rabbit erythrocytes loaded with Fluo-4 AM (5 μM) were treated with ProHlyA or HlyA and image acquisition and fluorescence-data analysis performed on an ImageStream® MkII imaging cytometer (N = 10,000). The histograms plot the frequency of events (*i. e.*, the passage of cells) on the *ordinates* as a function of the Fluo-4–fluorescence-signal intensity in arbitrary units on the *abscissas* for untreated cells (Control) and erythrocytes after 10 and 40 min of exposure to 70 or 7 nM of ProHlyA (upper row) or HlyA (lower row), respectively (indicated above the figures). The histogram corresponding to cells after 40 min of interaction with ProHlyA with the subsequent addition of 5 μM of ionomycin (Iono) is also shown as a control of Fluo-4 loading (upper row, extreme right figure). Bright-field (gray background) and fluorescence (black background; excitation at 488 nm) images of rabbit erythrocytes corresponding to each fluorescence distribution in the histograms are shown as *insets* placed beside (with a single peak) or directly above (with double peaks or triple peaks) the respective fluorescence distribution. The results are representative of two independent experiments with blood from two different animals.

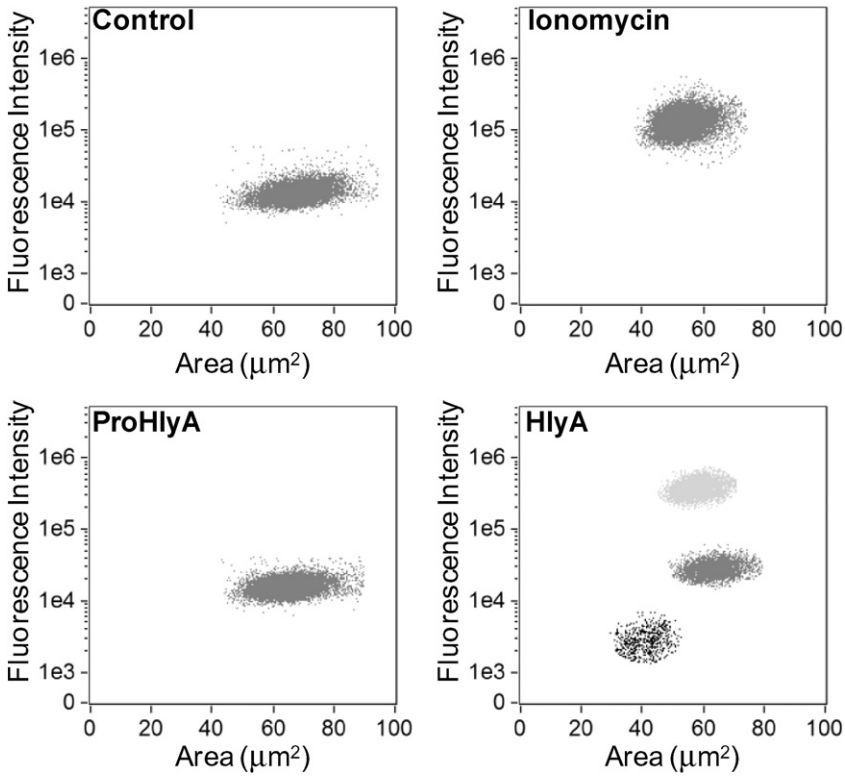


**Fig. 4.** Fluorescence intensity and area analysis in HlyA- and ProHlyA-treated erythrocytes. In the figures, the total fluorescence intensity in arbitrary units per cell is plotted as a function of the area (in $\mu m^2$) for each cell measured in the ImageStream® MkII imaging cytometer. Each dot represents a single erythrocyte. The figure show the plots for untreated erythrocytes (Control; left, upper row), cells after 40 min of exposure to ProHlyA (70 nM; left, lower row) or HlyA (7 nM right, lower row) as well as for ProHlyA-treated erythrocytes after the addition of 5 μM of ionomycin (right, upper row). The figures are representative of two independent experiments with blood from two different animals.

$Ca^{2+}$ (Fig. 5, Panel B). Control experiments with untreated erythrocytes in the presence of $Ni^{2+}$ or BBG underwent no changes in Fluo-4 fluorescence or cell morphology over time, thus confirming that those cellular responses were induced by the toxin (Supplementary Fig. 1). These results pointed out that a $Ca^{2+}$ entry was triggered by HlyA treatment through pathways that could not be blocked by those compounds. Thus,

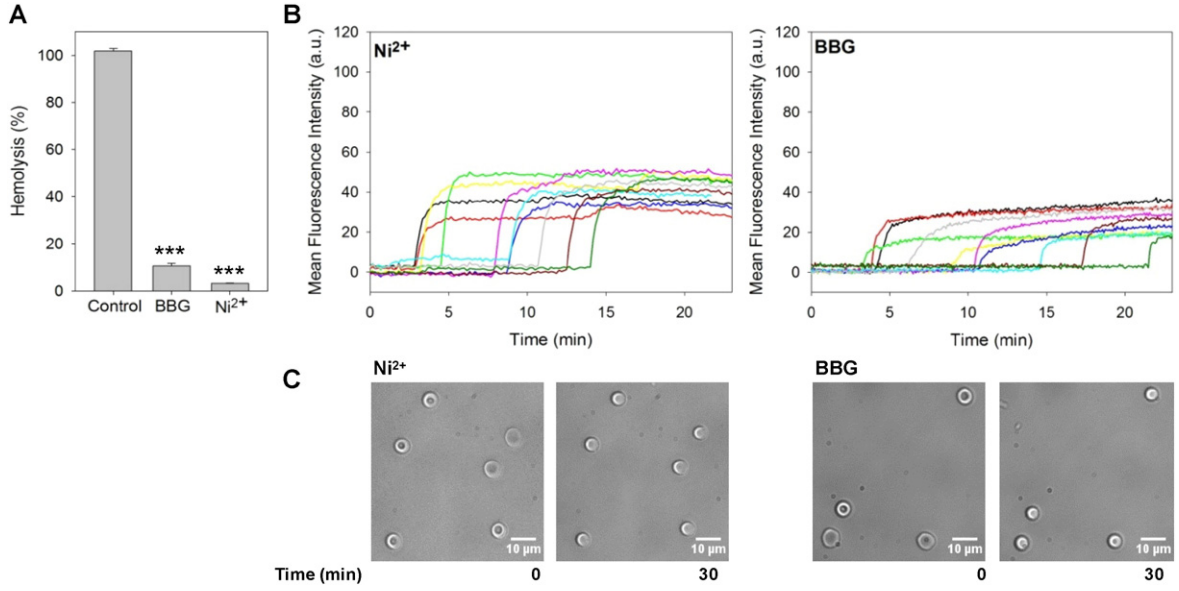


**Fig. 5.** Effects of $Ca^{2+}$-channel inhibitors on HlyA activity. Panel A: Hemolytic activity of 5 nM HlyA in rabbit erythrocytes after 30 min of exposure in the absence (Control) or presence of $Ca^{2+}$-channels inhibitors: the P2 antagonist Brilliant Blue G (BBG) at 10 μM or the voltage-gated–$Ca^{2+}$-channel blocker $Ni^{2+}$ at 2 mM. In the figure, the percent hemolysis is plotted on the *ordinate* for each of the experimental conditions indicated on the *abscissa*. The data represent the mean values ± SEM of 3 independent experiments with blood from 2 different rabbits as analyzed statistically by the Student *t*-test (***$p < 0.001$ compared to control values). Panel B: Erythrocytes treated with 5 nM HlyA in the presence of 2 mM $Ni^{2+}$ (left figure) or 10 μM BBG (right figure). Each record corresponds to the mean fluorescence intensity of single cells (colored curves) in arbitrary units per cell (corrected for background fluorescence), as designated on the *ordinate*, followed over the time in min indicated on the *abscissa*. The two figures present records representative of 4 independent experiments with blood from two different rabbits. Panel C: Bright-field images of rabbit erythrocytes before (time 0) and 30 min after the addition of 5 nM HlyA in the presence of 2 mM $Ni^{2+}$ (left field) or 10 μM BBG (right field).

our data strongly suggests that only the second increase, the one that might be related to an activation of purinergic channels, is responsible for cell lysis.

### 3.3. The effect of exogenous ATP on ProHlyA-treated erythrocytes

The results thus far have indicated that an activation of purinergic receptors is responsible for the second elevation in $Ca^{2+}$ concentration, an increase that is necessary for the occurrence of hemolysis in rabbit erythrocytes. Skals et al. have proposed that the interaction of HlyA alone destabilized the membrane, thus inducing an ATP efflux through the pore formed by the toxin, and that this ATP efflux was responsible for the $Ca^{2+}$-signal amplification through activation of purinergic receptors [30]. That the interaction of ProHlyA with the erythrocyte membrane does not produce cell lysis has been well established. Indirect evidence has suggested that the lack of oligomerization and pore formation might be responsible for this hemolytic inactivity [13]. Following this idea, we added exogenous ATP to ProHlyA-treated erythrocytes in order to test if the membrane perturbation induced by the protoxin, even though insufficient to induce any $Ca^{2+}$ influx *per se*, could nevertheless lead to hemolysis in the presence of exogenous ATP. The results demonstrated that the addition of exogenous ATP produced a slight degree of hemolysis in ProHlyA-treated erythrocytes, although no statistically significant differences in the hemolytic activity were found in the presence of 1 or 3 mM ATP compared to control experiments without ATP. The hemolysis produced by 8 nM ProHlyA was increased from 0.6 ± 0.3% in control experiments to 1.2 ± 0.4% and 1.6 ± 0.8% by the presence of 1 and 3 mM ATP, respectively. Notwithstanding, this increment in hemolysis is far from being similar to the marked lytic activity reported for exposure to 1 nM HlyA, which concentration already produced a 100% erythrocyte lysis (Fig. 1, Panel A). These results indicate that the interaction of ProHlyA with the membrane induces changes in the erythrocyte morphology; but, unlike the altered state affected by HlyA, the ProHlyA conformational structure is still not adequate either to form that putative pore or to activate any transduction pathway that could finally lead to hemolysis.

### 3.4. Interaction of HlyA and ProHlyA with lipid monolayers

Lipid monolayers are extremely useful for studying lipid-protein interactions because those model membranes permit a control of the surface pressure and lipid density along with the subphase content and lipid composition. HlyA interaction with such membrane models allowed the study of the adsorption and insertion phenomena in the absence of further changes in the lipid architecture because the monolayer could not undergo the three-dimensional membrane restructuring essential for altering the membrane-permeability barrier [14]. In the following experiments the increase in surface pressure (Δπ) caused by the interaction of HlyA or ProHlyA interaction with a monolayer composed of DOPC:SM:Chol at a lateral pressure of 20 mN/m was measured (Fig. 6). This lipid mixture was chosen since it represents a lipid composition similar to that of the outer hemilayer of erythrocyte membranes, as reported by us earlier [31,32]. In this model experimental system, both proteins accordingly produced an increase in surface pressure in the DOPC:SM:Chol monolayers at an initial lateral pressure of 20 mN/m. The total surface pressure increment achieved after the injection of 40 nM of either protein was 3.1 ± 0.4 and 3.0 ± 0.6 mN/m for HlyA and ProHlyA, respectively (Fig. 6).

These results suggest that despite the lack of lytic activity of ProHlyA, the effect of the protoxin's physical interaction with the erythrocyte membrane measured in terms of the resulting increment in surface pressure was similar to that obtained for HlyA.

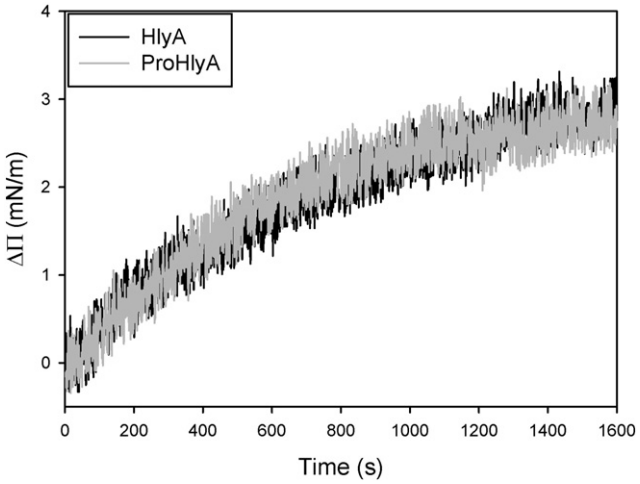


**Fig. 6.** Protein interaction with DOPC:SM:Chol monolayers. Time course of the interaction of HlyA (black line) or ProHlyA (gray line) with lipid monolayers of DOPC/16:0-SM/Chol in a 2:1:1 M ratio at an initial lateral pressure of 20 mN/m. The increase in surface pressure was monitored after the injection of 40 nM final concentration of the proteins into the buffer-containing subphase (20 mM Tris, 150 mM NaCl, 2 mM $CaCl_2$, pH 7.4). The experiments were performed at 20 ± 1 °C. In the figure—consisting of representative curves from 3 independent experiments—the increase in the monolayer's surface pressure, Δπ, in mN/m is plotted on the *ordinate* as a function of time in seconds on the *abscissa*.

## 4. Discussion

The *E.coli* HlyA is considered the prototype of the RTX family of toxins. Members of this family share many structural characteristics, among which is the acylation of internal lysine residues [5,33]. In the example of HlyA, the protoxin, ProHlyA, is matured in the cytosol to the active form by HlyC-directed fatty acylation at the ε-amino groups of the Lys 564 and Lys 690; which modification changes the benign protoxin to a frank toxin, before export from the producing bacteria. Up to the present, ProHlyA has been considered a strictly benign precursor, since the protoxin is hemolytically and cytolytically inactive [34,35], even though ProHlyA has been found capable of binding to erythrocytes to the same extent as HlyA [13,16]. In the present work, we have demonstrated for the first time that the interaction of ProHlyA with the erythrocyte membrane causes crenation of the cells independently of a $Ca^{2+}$ influx (Figs. 1–3). These findings have significant implications since the increase in $Ca^{2+}$ levels in HlyA-treated erythrocytes, along with the subsequent activation of the Gardos channels, has been largely considered to be responsible for the subsequent erythrocyte shrinkage and crenation [19]. The results obtained here, however, indicate that the mere interaction of ProHlyA with the membrane causes these morphologic changes since the unacylated precursor was not capable of inducing any $Ca^{2+}$ elevation in erythrocytes. The studies reported here on protein-lipid interactions through the use of lipid monolayers as membrane model systems demonstrated that ProHlyA produced increases in the surface pressure of lipid mixtures mimicking the outer leaflet of rabbit-erythrocytes membranes similar to the elevations effected by HlyA (Fig. 6). Moreover, in the absence of $Ca^{2+}$ (Fig. 2, Panel D), cell crenation was still observed in HlyA-treated erythrocytes, thus reinforcing the notion that $Ca^{2+}$ influx is not strictly required for the early morphologic changes that convert the discocytic erythrocyte into an echinocytic shape. All these findings support the interpretation that protein-membrane interactions *per se* may be responsible for the erythrocyte crenation induced by both proteins.

In a very recent work we demonstrated that the increase in intracellular $Ca^{2+}$ induced by HlyA, activated calpains responsible for the proteolysis of spectrins, ankyrin, Band 3, and protein 4.1. [22]. At that time, we proposed that the destabilization of the cytoskeleton might induce the shrinkage of the erythrocytes. The results presented here indicated

that the mere interaction of either protein with the erythrocyte membrane induced crenation of the cells since both proteins triggered those cellular morphologic alterations; even though ProHlyA did not produce any $Ca^{2+}$ influx, an indispensable condition for activating calpains [36]. Nevertheless, the entry of $Ca^{2+}$ ions that occurs after HlyA-treatment of erythrocytes may contribute to these morphologic changes through the activation of calpains and the subsequent signalling cascades that lead to membrane cytoskeleton destabilization and the spherocyte shape.

The monolayer technique is a widely used tool for studying protein-membrane interactions. On the basis of studies on a series of proteins with different tertiary structures, the increase in surface pressure of a lipid monolayer has been postulated to result from either the insertion of proteins or a conformational rearrangement of the proteins and lipids in the adsorbed layer [37]. Therefore, the findings obtained here for the interaction of HlyA and ProHlyA with these model membranes must not be considered as a direct indication of similar interactions on the part of both proteins with the lipid monolayers. Even though HlyA and ProHlyA both contain an amphipathic N-terminal region that may allow the interaction of either protein with the membrane, the two have one main structural difference: the presence of two fatty acids in the former. As we have demonstrated before, both proteins present different conformational structures in solution: HlyA exhibits a molten globule conformation, promoted by the presence of the covalently bound fatty acids; whereas ProHlyA assumes a more compact structure [38]. Therefore, both proteins may interact with the membrane in different tertiary conformations; and thus, even though the changes in surface pressure observed by the monolayer technique are similar, the nature of the membrane perturbation —*i. e.*, the number and extent of monomers inserted, the type of protein and lipid rearrangements, or other alterations—produced by the two proteins might still be different. Thus, differences in the interaction of both proteins with the erythrocyte membrane may certainly have discrepant implications in the final effect produced. While the interaction of HlyA may lead to an activation of transduction pathways that terminate in cell lysis, this same active membrane conformation might not be attained by association with ProHlyA, with only the early membrane-shape transitions occurring in the absence of any triggering of further signalling cascades.

In order to explain the shape alterations induced by HlyA and ProHlyA, the latter being independent of calcium influx, we revised the bilayer-couple hypothesis formulated by Sheetz and Singer [39,40]. According to their hypothesis, membranes forming a closed surface, whose proteins and polar lipids are asymmetrically distributed in the two halves of the membrane bilayer, can act as bilayer couples—that is, the two monolayers can respond differently to a perturbation while remaining coupled to one another, with the observed shape alterations arising from a differential expansion of the two monolayers of the lipid membrane. Echinocytogenic amphiphiles are thought to be equilibrated mainly in the outer monolayer so as to expand it with respect to the inner, whereas stomatogenic amphiphiles are considered to interact mainly with the inner monolayer, thus expanding it relative to the outer. Both HlyA and ProHlyA have been clearly shown to stabilize the echinocyte shape, thus indicating that both proteins intercalate preferentially in the outer monolayer. These present findings are in agreement with the results reported previously by Soloaga et al. using freeze–fracture electron microscopy of HlyA-treated liposomes [41]. On the basis of their results, they postulated that HlyA acts as a nontransmembrane intrinsic protein that induces a transient bilayer breakdown so as to result in a leakage of liposome contents. This mechanism could apply to the destabilization of erythrocyte membranes as well. Nevertheless, in contrast to membrane model systems, in the complex biologic environment of the living-cell membrane many different signalling pathways could be activated by the interaction of the toxin that could account for the responses observed here.

Time-lapse analysis revealed differential shape transitions in HlyA- and ProHlyA-treated erythrocytes. ProHlyA stabilized the echinocytic shape of erythrocytes with no further changes in morphology being observed thereafter. In contrast, HlyA induced spherocytosis before the hemolysis of rabbit erythrocytes occurred. The discocyte-echinocyte-spherocyte sequence of morphologic changes observed for HlyA is the same one occurring with amphiphiles that induce exovesicle formation [42,43]. Within this context, the release of exovesicles by platelets has been demonstrated to be commonly induced by stimuli leading to a rise in intracellular $Ca^{2+}$ and cytoskeleton remodelling through calpain activation [44]. These effects, together with a loss of membrane asymmetry, lead to an outward budding of exovesicles from the membrane (*cf.* the review in reference [45]). In addition, ATP binding to P2X7 receptors on myeloid cells has been shown to stimulate the excretion of such vesicles [46]. All these events —*i. e.*, the binding of ATP to P2X7 receptors, the increase in intracellular-$Ca^{2+}$ levels, and the calpain activation, among others—have been recently characterized by many research groups including ourselves (*cf.* Figs. 2 and 3) in HlyA-treated erythrocytes [23,22,19]. Thus, the possibility that the interaction of HlyA with the erythrocyte membrane may be triggering the excretion of these vesicles should not be discarded, though that hypothesis needs further investigation.

Regarding the role of $Ca^{2+}$, an influx of that cation occurs in a biphasic manner in HlyA-treated cells, with a first step-like increment followed by a second increase that continues to rise until lysis occurs, as reported previously [23] and also investigated further here (Fig. 2). In the present work we have furthermore demonstrated that the second $Ca^{2+}$ elevation decreased, along with hemolysis, when the $Ca^{2+}$ channels were inhibited by channel blockers like $Ni^{2+}$ or BBG (Fig. 5), thus confirming that an activation of endogenous $Ca^{2+}$ channels is needed for the lysis of rabbit erythrocytes. Skals et al. have recently proposed that the ATP efflux through toxin pores in the erythrocyte membrane is responsible for the activation of purinergic channels [30]. Little information is available in the literature regarding the purinergic receptors expressed in rabbit erythrocytes. Within this context, we assume that, as in other mammalian erythrocytes, the rabbit cells could express both ligand-gated ion channels—*i. e.*, the P2X and G protein-coupled (P2Y) receptors [47,48]. Skals et al. have proposed that the P2X7 proteins are the activated purinergic receptors in human erythrocytes treated with HlyA [20], at a $K_{0.5}$ of 100–300 μM for the ATP ligand [49]. The results obtained here indicate that, as in human erythrocytes [20], so in rabbit erythrocytes, purinergic receptors are involved in the amplification of the hemolytic process produced by HlyA, with those purinergic channels being responsible in the rabbit erythrocytes for the acute increase in intracellular $Ca^{2+}$ that ends in cell lysis. We need to emphasize at this point, that an increase in the extracellular ATP content is not in itself enough to produce the massive hemolysis observed after HlyA insertion since incubation with ATP caused only a modest increase in cell lysis in ProHlyA-treated erythrocytes. In addition to a purinergic-signalling amplification, the first increase in $Ca^{2+}$ levels triggered by the toxin could not be inhibited by the $Ca^{2+}$-channel blockers tested, thus indicating that a different pathway was responsible for that first step-like $Ca^{2+}$ increase that occurred after exposure to the toxin. HlyA is widely assumed to form pores of approximately 2 to 3 nm in diameter in the membrane that could account for the initial $Ca^{2+}$ entry observed, although this information is based on indirect measurements derived from osmotic-protection experiments and electrophysiological studies [50–52]. In fact, electron microscopy, crystal-structure analysis, and other techniques have failed to directly reveal the pores formed by HlyA, so that the existence of such a toxin pore in the target-cell membrane still remains controversial. One probable difficulty in observing such a pore could be the formation of highly dynamic structures of a proteolipidic nature by HlyA, whose conductance and membrane lifetime would be dependent on the membrane-lipid composition, as has been proposed by Bakás et al. [53].

Fatty acids covalently bound to the toxin have been considered to be responsible for inducing a molten-globule conformation in the protein that may favor protein-protein interactions along with the occurrence

of oligomerization and possible pore formation [13,38]. Considering all these aspects, and taking into account the results obtained here for HlyA and ProHlyA, we are tempted to propose that the first increase in $Ca^{2+}$ levels in HlyA-treated erythrocytes might occur as a result of the HlyA-specific nature of the perturbation induced by this toxin in the erythrocyte membrane, since ProHlyA could not effect that initial elevation. That first $Ca^{2+}$ influx could be counteracted by the $Ca^{2+}$ effluxes from the cell since only when the purinergic receptors are activated, does the sustained $Ca^{2+}$ entry through these channels produce the ionic imbalance that finally ends in cell swelling and erythrocyte lysis. Nevertheless, when no $Ca^{2+}$ influx through purinergic channels occurs, the erythrocytes stay in a spherocyte shape.

In summary; the results presented here indicate that both proteins, the hemolytically active HlyA and the inactive ProHlyA, induce cell crenation in rabbit erythrocytes, with this transformation being a $Ca^{2+}$-independent phenomenon: the mere interaction of the proteins with the erythrocyte membrane induces morphologic changes in the cell. Within this context, both proteins could intercalate in the outer monolayer of the rabbit-erythrocyte membrane so as to produce the discocyte-to-echinocyte–shape transition. Nevertheless, only HlyA, the acylated toxin–through membrane destabilization and/or the activation of transductional pathways–can affect the influx of $Ca^{2+}$, and presumably the release of exovesicles, that lead to an intermediate spherocyte shape and finally a swelling and lysis as a result of the massive entry of the cation through purinergic channels.

Supplementary data to this article can be found online at http://dx.doi.org/10.1016/j.bbamem.2016.05.013.

## Transparency document

The Transparency document associated with this article can be found, in the online version.

## Authors' contributions

RV performed all the experiments. CMG performed the flow cytometer assays. RV, CMG, SM, LB, and VH planned the experiments; analyzed the experimental data; and wrote the manuscript.

## Acknowledgements

We thank Elizabeth Mata and the laboratory-animal facility of the Instituto de Biotecnología, UNAM for assistance with animal care and sample collection. We also thank Andrés Saraleguí Amaro, staff member of the Laboratorio Nacional de Microscopía Avanzada, UNAM for helping us with the flow cytometer.

RV wishes to thank Red de Macrouniversidades postgraduate mobility program for financial support. This work was supported by the Agencia Nacional de Promoción Científica y Tecnológica [grant number PICT 2657/2013], Universidad Nacional de La Plata [grant number M11/181] and MINCyT-CONACyT bilateral cooperation [grant number MX1320].

R.V. is a fellow of the Consejo Nacional de Investigaciones Científicas y Técnicas (CONICET), Argentina. L.B. and S.M. are members of the Carrera del Investigador Comisión de Investigaciones Científicas de la Provincia de Buenos Aires (CICBA), Argentina. V.H. is a member of the Carrera del Investigador of CONICET. R.V., S.M., L.B. and V.H. are members of the Iberoamerican CYTED Network BIOTOX 212RT0467.

Dr. Donald F. Haggerty, a retired academic career investigator and native English speaker, edited the final version of the manuscript.

## References

[1] G. Nagy, A. Altenhoefer, O. Knapp, E. Maier, U. Dobrindt, G. Blum-Oehler, R. Benz, L. Emody, J. Hacker, Both alpha-haemolysin determinants contribute to full virulence of uropathogenic *Escherichia coli* strain 536, Microbes Infect. 8 (2006) 2006–2012.
[2] J.R. Johnson, Virulence factors in *Escherichia coli* urinary tract infection, Clin. Microbiol. Rev. 4 (1991) 80–128.
[3] L.C. Ristow, R.A. Welch, Hemolysin of uropathogenic *Escherichia coli*: a cloak or a dagger? Biochim. Biophys. Acta 1858 (2015) 538–545.
[4] L. Bakás, S. Maté, R. Vazquez, V. Herlax, *E. coli* alpha hemolysin and properties, in: P.D. Ekinci (Ed.), Biochemistry, Book I, 2012 (Croacia).
[5] I. Linhartova, L. Bumba, J. Masin, M. Basler, R. Osicka, J. Kamanova, K. Prochazkova, I. Adkins, J. Hejnova-Holubova, L. Sadilkova, J. Morova, P. Sebo, RTX proteins: a highly diverse family secreted by a common mechanism, FEMS Microbiol. Rev. 34 (2010) 1076–1112.
[6] C. Wandersman, P. Delepelaire, TolC, an *Escherichia coli* outer membrane protein required for hemolysin secretion, Proc. Natl. Acad. Sci. U. S. A. 87 (1990) 4776–4780.
[7] T. Felmlee, S. Pellett, E.Y. Lee, R.A. Welch, *Escherichia coli* hemolysin is released extracellularly without cleavage of a signal peptide, J. Bacteriol. 163 (1985) 88–93.
[8] J. Issartel, V. Koronakis, C. Hughes, Activation of *Escherichia coli* prohaemolysin to the mature toxin by acyl carrier protein-dependent fatty acylation, Nature 351 (1991) 759–761.
[9] V. Koronakis, J. Li, E. Koronakis, K. Stauffer, Structure of TolC, the outer membrane component of the bacterial type I efflux system, derived from two-dimensional crystals, Mol. Microbiol. 23 (1997) 617–626.
[10] P. Stanley, L. Packman, V. Koronakis, C. Hughes, Fatty acylation of two internal lysine residues required for the toxic activity of *Escherichia coli* hemolysin, Science 266 (1994) 1992–1996.
[11] L.M. Worsham, M.S. Trent, L. Earls, C. Jolly, M.L. Ernst-Fonberg, Insights into the catalytic mechanism of HlyC, the internal protein acyltransferase that activates *Escherichia coli* hemolysin toxin, Biochemistry 40 (2001) 13607–13616.
[12] L.M. Worsham, K.G. Langston, M.L. Ernst-Fonberg, Thermodynamics of a protein acylation: activation of *Escherichia coli* hemolysin toxin, Biochemistry 44 (2005) 1329–1337.
[13] V. Herlax, S. Mate, O. Rimoldi, L. Bakas, Relevance of fatty acid covalently bound to *Escherichia coli* alpha-hemolysin and membrane microdomains in the oligomerization process, J. Biol. Chem. 284 (2009) 25199–25210.
[14] L. Sanchez-Magraner, A. Cortajarena, F. Goni, H. Ostolaza, Membrane insertion of *Escherichia coli* alpha-hemolysin is independent from membrane lysis, J. Biol. Chem. 281 (2006) 5461–5467.
[15] P. Stanley, V. Koronakis, C. Hughes, Acylation of *Escherichia coli* hemolysin: a unique protein lipidation mechanism underlying toxin fuction, Microbiol. Mol. Biol. Rev. 62 (1998) 309–333.
[16] M.E. Bauer, R.A. Welch, Association of RTX toxins with erythrocytes, Infect. Immun. 64 (1996) 4665–4672.
[17] A. Valeva, I. Walev, H. Kemmer, S. Weis, I. Siegel, F. Boukhallouk, T. Wassenaar, T. Chavakis, S. Bhakdi, Binding of *Escherichia coli* hemolysin and activation of the target cells is not receptor-dependent, J. Biol. Chem. 280 (2005) 36657–36663.
[18] D. Boehm, R. Welch, I. Snyder, Domains of *Escherichia coli* hemolysin (HlyA) involved in binding of calcium and erythrocyte membranes, Infect. Immun. 58 (1990) 1959–1964.
[19] M. Skals, U. Jensen, J. Ousingsawat, K. Kunzelmann, J. Leipziger, H. Praetorius, *Escherichia coli* alpha-hemolysin triggers shrinkage of erythrocytes via K(Ca)3.1 and TMEM16A channels with subsequent phosphatidylserine exposure, J. Biol. Chem. 285 (2010) 15557–15565.
[20] M. Skals, N.R. Jorgensen, J. Leipziger, H.A. Praetorius, Alpha-hemolysin from *Escherichia coli* uses endogenous amplification through P2X receptor activation to induce hemolysis, Proc. Natl. Acad. Sci. U. S. A. 106 (2009) 4030–4035.
[21] M. Skals, H.A. Praetorius, Mechanisms of cytolysin-induced cell damage — a role for auto- and paracrine signalling, Acta Physiol (Oxford) 209 (2013) 95–113.
[22] F.C. Velasquez, S. Mate, L. Bakas, V. Herlax, Induction of eryptosis by low concentrations of *E. coli* alpha-hemolysin, Biochim. Biophys. Acta 1848 (2015) 2779–2788.
[23] S. Sanchez, L. Bakás, E. Gratton, V. Herlax, Alpha hemolysin induces an increase of erythrocytes calcium: a FLIM 2-photon phasor analysis approach, PLoS One 6 (6) (2011) e21127.
[24] M. Moayeri, R. Welch, Prelytic and lytic conformation of erythrocyte-associated *Escherichia coli* hemolysin, Infect. Immun. 65 (1997) 2233–2239.
[25] R. Vazquez, S. Maté, L. Bakás, M. Fernández, E. Malchiodi, V. Herlax, Novel evidence for the specific interaction between cholesterol and α-haemolysin of *Escherichia coli*, Biochem. J. 458 (2014) 481–489.
[26] A.W. Jay, Geometry of the human erythrocyte. I. Effect of albumin on cell geometry, Biophys. J. 15 (1975) 205–222.
[27] W.S. Rasband, ImageJ: National Institutes of Health, Bethesda, Maryland, USA, 1997-2014.
[28] S.E. Jorgensen, R.F. Hammer, G.K. Wu, Effects of a single hit from the alpha hemolysin produced by *Escherichia coli* on the morphology of sheep erythrocytes, Infect. Immun. 27 (1980) 988–994.
[29] C.K. Larsen, M. Skals, T. Wang, M.U. Cheema, J. Leipziger, H.A. Praetorius, Python erythrocytes are resistant to alpha-hemolysin from *Escherichia coli*, J. Membr. Biol. 244 (2011) 131–140.
[30] M. Skals, R.G. Bjaelde, J. Reinholdt, K. Poulsen, B.S. Vad, D.E. Otzen, J. Leipziger, H.A. Praetorius, Bacterial RTX toxins allow acute ATP release from human erythrocytes directly through the toxin pore, J. Biol. Chem. 289 (2014) 19098–19109.
[31] S. Mate, J.V. Busto, A.B. Garcia-Arribas, J. Sot, R. Vazquez, V. Herlax, C. Wolf, L. Bakas, F.M. Goni, N-nervonoylsphingomyelin (C24:1) prevents lateral heterogeneity in cholesterol-containing membranes, Biophys. J. 106 (2014) 2606–2616.
[32] S.M. Mate, R.F. Vazquez, V.S. Herlax, M.A. Daza Millone, M.L. Fanani, B. Maggio, M.E. Vela, L.S. Bakas, Boundary region between coexisting lipid phases as initial binding sites for *Escherichia coli* alpha-hemolysin: a real-time study, Biochim. Biophys. Acta 1838 (2014) 1832–1841.

[33] R. Welch, RTX toxin structure and function: a story of numerous anomalies and few analogies in toxin biology, Curr. Top. Microbiol. Immunol. 257 (2001) 85–111.
[34] A. Soloaga, H. Ostolaza, F. Goñi, F. De la Cruz, Purification of *Escherichia coli* prohaemolysin, and a comparison with the properties of mature α-haemolysin, Eur. J. Biochem. 238 (1996) 418–422.
[35] S. Pellet, R. Welch, *Escherichia coli* hemolysin mutants with altered target cell specificity, Infect. Immun. 64 (1996) 3081–3087.
[36] T. Murachi, Calcium-dependent proteinases and specific inhibitors: calpain and calpastatin, Biochem. Soc. Symp. 49 (1984) 149–167.
[37] R. Maget-Dana, The monolayer technique: a potent tool for studying the interfacial properties of antimicrobial and membrane-lytic peptides and their interactions with lipid membranes, Biochim. Biophys. Acta 1462 (1999) 109–140.
[38] V. Herlax, L. Bakas, Fatty acids covalently bound to alpha-hemolysin of *Escherichia coli* are involved in the molten globule conformation: implication of disordered regions in binding promiscuity, Biochemistry 46 (2007) 5177–5184.
[39] M.P. Sheetz, S.J. Singer, Biological membranes as bilayer couples. A molecular mechanism of drug–erythrocyte interactions, Proc. Natl. Acad. Sci. U. S. A. 71 (1974) 4457–4461.
[40] M.P. Sheetz, R.G. Painter, S.J. Singer, Biological membranes as bilayer couples. III. Compensatory shape changes induced in membranes, J. Cell Biol. 70 (1976) 193–203.
[41] A. Soloaga, M.P. Veiga, L.M. García-Segura, H. Ostolaza, R. Brasseur, F.M. Goñi, Insertion of *Escherichia coli* α-haemolysin in lipid bilayer as a non-transmembrane integral protein:prediction and experiment, Mol. Microbiol. 31 (1999) 1013–1024.
[42] H. Hagerstrand, B. Isomaa, Vesiculation induced by amphiphiles in erythrocytes, Biochim. Biophys. Acta 982 (1989) 179–186.
[43] H. Hagerstrand, B. Isomaa, Morphological characterization of exovesicles and endovesicles released from human erythrocytes following treatment with amphiphiles, Biochim. Biophys. Acta 1109 (1992) 117–126.
[44] J.M. Pasquet, J. Dachary-Prigent, A.T. Nurden, Calcium influx is a determining factor of calpain activation and microparticle formation in platelets, Eur. J. Biochem. 239 (1996) 647–654.
[45] B. Hugel, M.C. Martínez, C. Kunzelmann, J.M. Freyssinet, Membrane microparticles: two sides of the coin, Physiology 20 (2005) 22–27.
[46] F. Bianco, E. Pravettoni, A. Colombo, U. Schenk, T. Moller, M. Matteoli, C. Verderio, Astrocyte-derived ATP induces vesicle shedding and IL-1β release from microglia, J. Immunol. 174 (2005) 7268–7277.
[47] G. Burnstock, Blood cells: an historical account of the roles of purinergic signalling, Purinergic Signal 11 (2015) 411–434.
[48] R. Sluyter, P2X and P2Y receptor signaling in red blood cells, Front. Mol. Biosci. 2 (2015) 60.
[49] M.F. Leal Denis, Homeostasis de ATP extracelular en eritrocitos: Interregulación y consecuencias funcionales, Instituto de Química y Fisicoquímica Biológicas- Facultad de Farmacia y Bioquímica, Universidad de Buenos Aires, Buenos Aires 2014, p. 171.
[50] M. Moayeri, R. Welch, Effects of temperature, time, and toxin concentration on lesion formation by the *Escherichia coli* hemolysin, Infect. Immun. 62 (10) (1994) 4124–4134.
[51] R. Benz, E. Maier, S. Bauer, A. Ludwig, The deletion of several amino acid stretches of *Escherichia coli* alpha-hemolysin (HlyA) suggests that the channel-forming domain contains beta-strands, PLoS One 9 (2014) e112248.
[52] M. Ropele, G. Menestrina, Electrical properties and molecular architecture of the channel formed by *Escherichia coli* hemolysin in planar lipid membranas, Biochim. Biophys. Acta 985 (1989) 9–18.
[53] L. Bakas, A. Chanturiya, V. Herlax, J. Zimmerberg, Paradoxical lipid dependence of pores formed by the *Escherichia coli* alpha-hemolysin in planar phospholipid bilayer membranes, Biophys. J. 91 (2006) 3748–3755.